Metabolic Engineering Communications 13 (2021) e00176

Contents lists available at ScienceDirect

Metabolic Engineering Communications

journal homepage: www.elsevier.com/locate/mec

Electronic signals are electrogenetically relayed to control cell growth and co-culture composition

Kristina Stephens [a,b,c], Fauziah Rahma Zakaria [a,b,c], Eric VanArsdale [a,b,c], Gregory F. Payne [b,c], William E. Bentley [a,b,c,*]

[a] Fischell Department of Bioengineering, University of Maryland, College Park, USA
[b] Institute for Bioscience and Biotechnology Research, University of Maryland, College Park, USA
[c] Robert E. Fischell Institute for Biomedical Devices, University of Maryland, College Park, USA

ARTICLE INFO

Keywords:
Electrogenetics
Quorum sensing
Cell-cell signaling
Microbiome
Internet-of-things

ABSTRACT

There is much to be gained by enabling electronic interrogation and control of biological function. While the benefits of bioelectronics that rely on potential-driven ionic flows are well known (electrocardiograms, defibrillators, neural prostheses, etc) there are relatively few advances targeting nonionic molecular networks, including genetic circuits. Redox activities combine connectivity to electronics with the potential for specific genetic control in cells. Here, electrode-generated hydrogen peroxide is used to actuate an electrogenetic "relay" cell population, which interprets the redox cue and synthesizes a bacterial signaling molecule (quorum sensing autoinducer AI-1) that, in turn, signals increased growth rate in a second population. The dramatically increased growth rate of the second population is enabled by expression of a phosphotransferase system protein, HPr, which is important for glucose transport. The potential to electronically modulate cell growth via direct genetic control will enable new opportunities in the treatment of disease and manufacture of biological therapeutics and other molecules.

1. Introduction

Synthetic biologists have engineered microbes to carry out wide-ranging functions in an array of applications (Cameron et al., 2014). Examples include microbes that detect hazardous molecules in environmental samples (Roggo and van der Meer, 2017; Cai et al., 2018; Kang et al., 2018), seek out a specific locale (McKay et al., 2017), and synthesize and secrete pathogen-specific toxins or disease-specific therapeutics in complex environments (Hwang et al., 2017; McKay et al., 2018). The power of these systems often lies in the cell's ability to synthesize a wide range of biological molecules, and to do so as programmed (at specific times, in response to specific environmental conditions, etc.). Notably, there has also been a rapid expansion of studies in which the function-triggering cue has not been an environmental factor or chemical, but a signal completely orthogonal to the metabolic activity of the host cells. For example, systems built on optical (Olson et al., 2014), magnetic (Stanley et al., 2015) and even electronic inputs have appeared (Tschirhart et al., 2017). These stimuli are particularly attractive in that they can be applied via external means, including for applications *in vivo* where adding a chemical inducer can be difficult or impossible. For instance, Stanley et al. developed a system for magnetically triggered release of insulin from mammalian cells (Stanley et al., 2015). We introduced electronic control of target gene expression by tapping into the switchable oxidation state of native redox active molecules (Tschirhart et al., 2017; Bhokisham et al., 2020). This allowed electronic access to an array of biological molecules or functions that can be synthesized or carried out by cells. This strategy expanded the capabilities of electronic systems, which are ubiquitous in modern society.

Electronic control of target gene expression using redox-active molecules is still in its infancy, however, with few examples that have appeared. Weber et al. electrochemically oxidized ethanol to acetaldehyde to regulate expression from an acetaldehyde-inducible promoter in mammalian cells (Weber et al., 2009). Krawczyk et al., developed transgene expression based on voltage-gated ionic currents for insulin release in diabetic mice (Krawczyk et al., 2020). To engineer electronic actuation of gene expression in bacteria, Tschirhart et al. coopted the SoxRS system (Tschirhart et al., 2017), which natively regulates the cell

* Corresponding author. Fischell Department of Bioengineering, 5102 Clark Hall, University of Maryland, College Park, MD, 20742, USA.
E-mail address: bentley@umd.edu (W.E. Bentley).

https://doi.org/10.1016/j.mec.2021.e00176
Received 28 January 2021; Received in revised form 20 May 2021; Accepted 31 May 2021
Available online 13 June 2021

oxidative stress response (Tsaneva and Weiss, 1990). The authors found that by using the redox-active molecule pyocyanin (Dietrich et al., 2008) and the mediator ferricyanide, *soxS* promoter activity could be controlled electrically. They demonstrated electronic control of both quorum sensing (QS) signaling and chemotaxis. Bhokisham et al., used a similar system for electronic control of CRISPR components in spatially-controlled environments (Bhokisham et al., 2020). More recently, Terrell et al. generated hydrogen peroxide at an electrode surface to regulate a gene of interest from the *oxyS* promoter (Terrell et al., 2021). That is, the OxyRS regulon is sensitive to hydrogen peroxide (Virgile et al., 2018; Rubens et al., 2016), which in turn can be generated at a gold electrode surface through reduction of oxygen (Qiang et al., 2002; Sanchez-Sanchez and Bard, 2009). By engineering cells so they could adhere to a gold electrode surface, they showed that an electrical signal could be imparted to a surface-bound population, transformed to a biological signal (bacterial autoinducer), and then emitted to second and third populations in the bulk media. The second population confirmed signal fidelity while the third population was programmed to release cargo, such as a GI tract biotherapeutic.

In parallel and in an analogous manner, synthetic biologists have also designed co-cultures and consortia to carry out desired functions wherein tasks are divided among subpopulations (Jawed et al., 2019). Each subtask of an overall function is built into an individual strain optimized to carry out a part of the whole. Then, optimized subpopulations are assembled so that the overall function is enabled from the component parts. These systems provide more design options and potentially more capability, but their compositions must be regulated. We showed how rewired bacterial quorum sensing could enable autonomous subpopulation control, based on endogenous signaling (Stephens et al., 2019).

Recognizing that compositional control might also benefit by the use of exogenous cues, in this work, we rewired the OxyRS system to enable electronic control of cell growth. To enable cell growth rate control of a target population, we chose to use an intermediate population that would first detect the electrically generated signal and convert that into a more stable, longer lasting signal that subsequently regulates the growth rate of the target population. Hence, our system consists of two cell populations (Fig. 1). The first population, the "relay" cells, detect hydrogen peroxide generated at a gold electrode, and produce bacterial autoinducer, AI-1. The specific AI-1 signal used here, N-3-oxo-dodecanoyl-L-homoserine lactone, is native to *Pseudomonas aeruginosa* (Miller and Bassler, 2001). This quorum sensing autoinducer has been widely used within synthetic biology systems that rely on cell-cell signaling because of its simplicity (i.e., one signal synthase, LasI, and a cognate transcriptional regulator, LasR) and well-characterized genetic control. Moreover, AI-1 freely diffuses through cell membranes, so the message can be carried to many cells. The second population that responds to the relayed signal and, in effect, controls the population profile, is referred to as the "controller" cells; they detect AI-1 (the signal relayed from the electrode) and grow faster in response. The relay cells, which detect hydrogen peroxide, are based on our previous work with cells that are adhered to a gold electrode (Terrell et al., 2021). Here, we altered the design by showing that these cells need not be adhered to a gold electrode but can translate hydrogen peroxide signals while in the bulk media. Importantly, the "relay" strain converts the hydrogen peroxide signal that is generated at the electrode, into a relatively more stable AI-1 signal. That is, *E. coli* rapidly consume hydrogen peroxide (Virgile et al., 2018), which is not the case with AI-1. The AI-1 signal is then dispersed throughout the bulk media (through stirring or shaking), where it regulates the growth of the "controller" strain. We used a slow-growing host as the relay strain so that the relayed signal generated at the electrode is imparted to the main population of interest (the controller strain) and the "relay" strain remains a minor constituent of the whole. We also chose to use the *P. aeruginosa* LasI-synthesized AI-1 as the intermediate signal, as this quorum sensing molecule can be easily produced by a small number of cells at high concentrations (relative to the concentration required for induction of the AI-1 promoter in the controller population). The "controller" strain was previously developed for AI-1 modulated cell growth by repurposing the phosphotransferase system (PTS) protein, HPr (Stephens et al., 2019), which is important in uptake of PTS sugars (such as glucose) into the cell (Deutscher, 2008). In that work, we showed that an engineered co-culture could detect the QS molecule AI-2 and autonomously adjust its culture composition through AI-1 signaling (Stephens et al., 2019). Here, we show that an external user can electrically modulate the growth rate of the controller strain and hence, the culture composition.

We first constructed and characterized the "relay" strain in a new host with attenuated growth and accentuated relay capabilities. Then, we co-culture the relay and controller strains, and demonstrate the ability to increase the growth rate of the controller strain by applying an electric potential using a gold electrode. In doing so, we also demonstrate electrical alteration of the resulting co-culture composition.

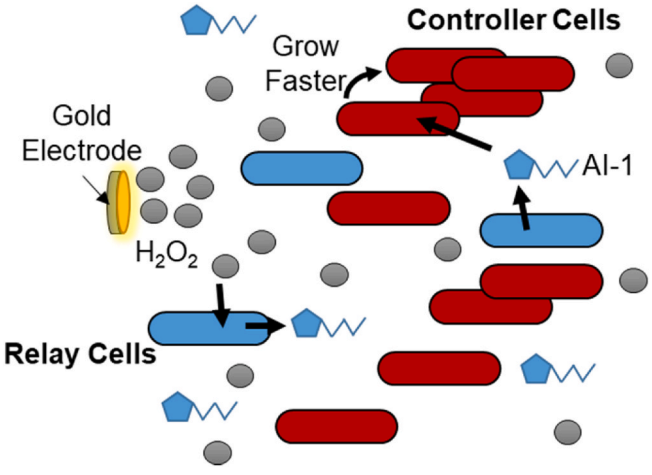

Fig. 1. Scheme for electronic control of cell growth rate through hydrogen peroxide generation.
Hydrogen peroxide is generated at the surface of a gold electrode. The "relay" cells (blue) detect hydrogen peroxide and synthesize AI-1 in response. The "controller" cells (red) detect AI-1 which activates production of HPr, enabling these cells to grow faster. (For interpretation of the references to colour in this figure legend, the reader is referred to the Web version of this article.)

2. Results

2.1. Design and characterization of the "relay" cell

The relay population was designed to detect hydrogen peroxide and respond by synthesizing AI-1. Plasmid pOxyRS-LasI (Terrell et al., 2021) contains *lasI*, which synthesizes AI-1 under the hydrogen peroxide-sensitive *oxyS* promoter (Fig. 2a) and is adapted from a vector designed for peroxide induced gene expression (Rubens et al., 2016). We previously modified *lasI* to incorporate a degradation tag (Andersen et al., 1998) at the C-terminus to limit AI-1 production after the hydrogen peroxide has been consumed (Terrell et al., 2021). In Fig. 2, we tested the *lasI* construct in the original NEB10β host, as well as a slow growing PH04 host. PH04 is a *ptsH* knockout derived from *E. coli* W3110 (Stephens et al., 2019; Ha et al., 2018), and is deficient in glucose uptake. We note that *ptsH* encodes the protein HPr. We hypothesized that by using PH04 as the host, the relay strain would not compete well with other populations for glucose in the media and would be less likely to overtake the culture if cultured with other populations. Here, we tested whether PH04 pOxyRS-LasI could synthesize AI-1 at sufficient levels to enable genetic control in engineered receiver cells ($>\sim$20 nM[23]). We compared AI-1 synthesis in both the PH04 and NEB10β hosts (Fig. 2b). Cultures were inoculated at a starting OD_{600} of 0.01 and 0–50 μM

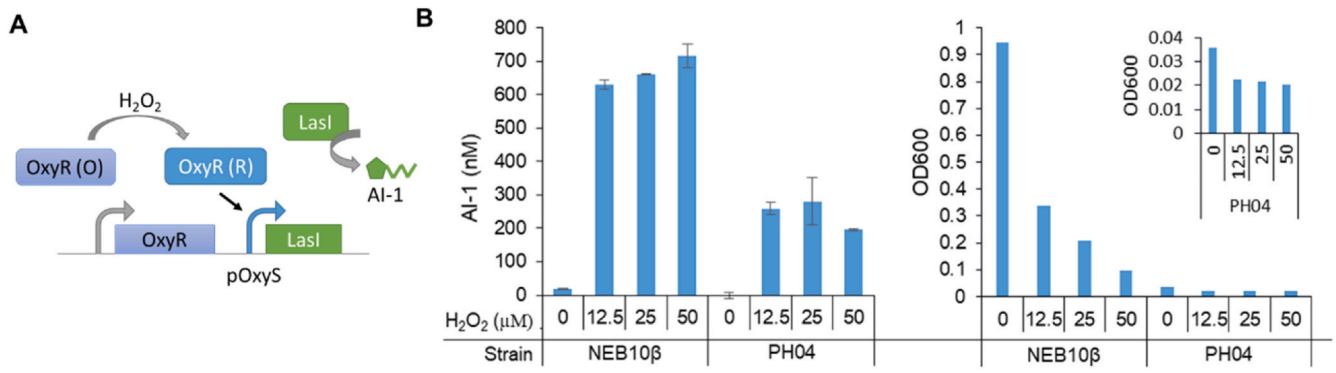

Fig. 2. Comparison of relay cell behavior in different host strains.
a) Scheme of peroxide-induced AI-1 from plasmid pOxyRS-LasI. Hydrogen peroxide reduces OxyR, which then activates the *oxyS* promoter and initiates transcription of *lasI* and subsequent synthesis of AI-1. **b)** NEB10β pOxyRS-LasI and PH04 pOxyRS-LasI were inoculated to a starting OD of 0.01. Hydrogen peroxide, ranging from 0 to 50 μM, was added to each culture as indicated. After 5.5 h of growth, samples were collected for measurement of AI-1 levels and cell density (OD_{600}). Error bars represent s.d. of technical duplicates. The small insert shows the cell density data for the PH04 strain with an expanded y-axis.

hydrogen peroxide was added. We chose to use 0–50 μM hydrogen peroxide, as previous results showed that 25 μM hydrogen peroxide resulted in strong activation of the *oxyS* promoter (Virgile et al., 2018). After 5.5 h, cell density was measured and conditioned media samples were collected for analysis of extracellular AI-1. This time frame was expected to be sufficient for the cells to both consume the hydrogen peroxide and produce AI-1 (Virgile et al., 2018). Hydrogen peroxide resulted in significant synthesis of AI-1 (as expected). PH04 cultures produced less AI-1 than NEB10β cultures. However, both strains produced sufficient AI-1 for signaling to a second population (previous results show that around 100 nM AI-1 produces the maximum response in the controller cells (Stephens et al., 2019)). Importantly, the PH04 relay cells grew to significantly lower cell densities over the 5.5 h than the NEB10β cells. PH04 densities ranged from OD 0.036 (0 μM H_2O_2) to 0.020 (50 μM H_2O_2), while NEB10β densities ranged from OD 0.94 to 0.10. We note that the insert shows the PH04 cell density data on an expanded y-axis to clearly see the effect of hydrogen peroxide on cell density in this strain. Hydrogen peroxide addition caused this drop in final cell density. In previous studies using a much higher starting cell density (approximately OD_{600} ~ 0.5 compared to OD_{600} ~ 0.01 used here), 50 μM hydrogen peroxide did not affect cell growth (Virgile et al., 2018). The difference here was likely due to the low initial cell density, which affects the rate of hydrogen peroxide consumption and hence, overall toxicity (Virgile et al., 2018). Although the cell density after 5 h is lower for higher hydrogen peroxide concentrations, it remains evident that the cells were highly activated as the AI-1 production remained high despite the lower cell density.

Next, we characterized AI-1 production in the PH04 relay strain over time for a range of hydrogen peroxide concentrations. We started with an initial OD_{600} of approximately 0.03, added 0–50 μM hydrogen peroxide, and collected samples to measure extracellular AI-1 every hour (Fig. 3a). Cultures without hydrogen peroxide produced little to no AI-1. Generally, higher concentrations of hydrogen peroxide resulted in higher synthesis of AI-1, and the majority of the AI-1 synthesis occurred within the first 2 h. We also measured cell density over time and found that the effects of hydrogen peroxide with a 0.03 initial OD_{600} had only a minimal effect on growth (Fig. 3b). This is contrary to Fig. 2, where similar hydrogen peroxide conditions decreased cell growth rate but with initial OD_{600} of ~0.01. Cells naturally consume and remove hydrogen peroxide. Starting with a higher cell density increases the rate of hydrogen peroxide removal and reduces the amount of hydrogen peroxide consumed on a per cell basis, which likely explains the toxicity of hydrogen peroxide at lower starting cell densities. These data reflect the transient nature of the initial hydrogen peroxide signal relative to the number of relay cells and the potential for influencing the subsequent AI-1 levels and signal propagation.

3. Electronic control of cell growth through peroxide generation

To demonstrate electronic control of cell growth rate, we co-cultured the relay cells, PH04 pOxyRS-LasI, with the growth controller cells, PH04 pAHL-HPr (Stephens et al., 2019) (Fig. 4). pAHL-HPr contains the

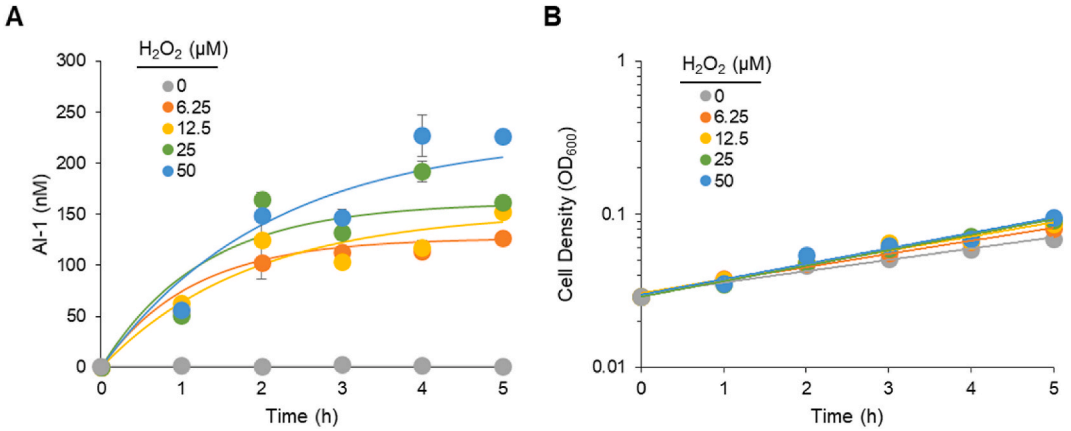

Fig. 3. AI-1 Production in relay cells over time
PH04 pOxyRS-LasI were inoculated to a starting OD of 0.03. A range of hydrogen peroxide concentrations were added to cultures as indicated ($t = 0$). Samples were collected for measurement of extracellular AI-1 (**a**) and cell density (OD600) (**b**) every 60 min. Error bars represent s.d. of technical duplicates.

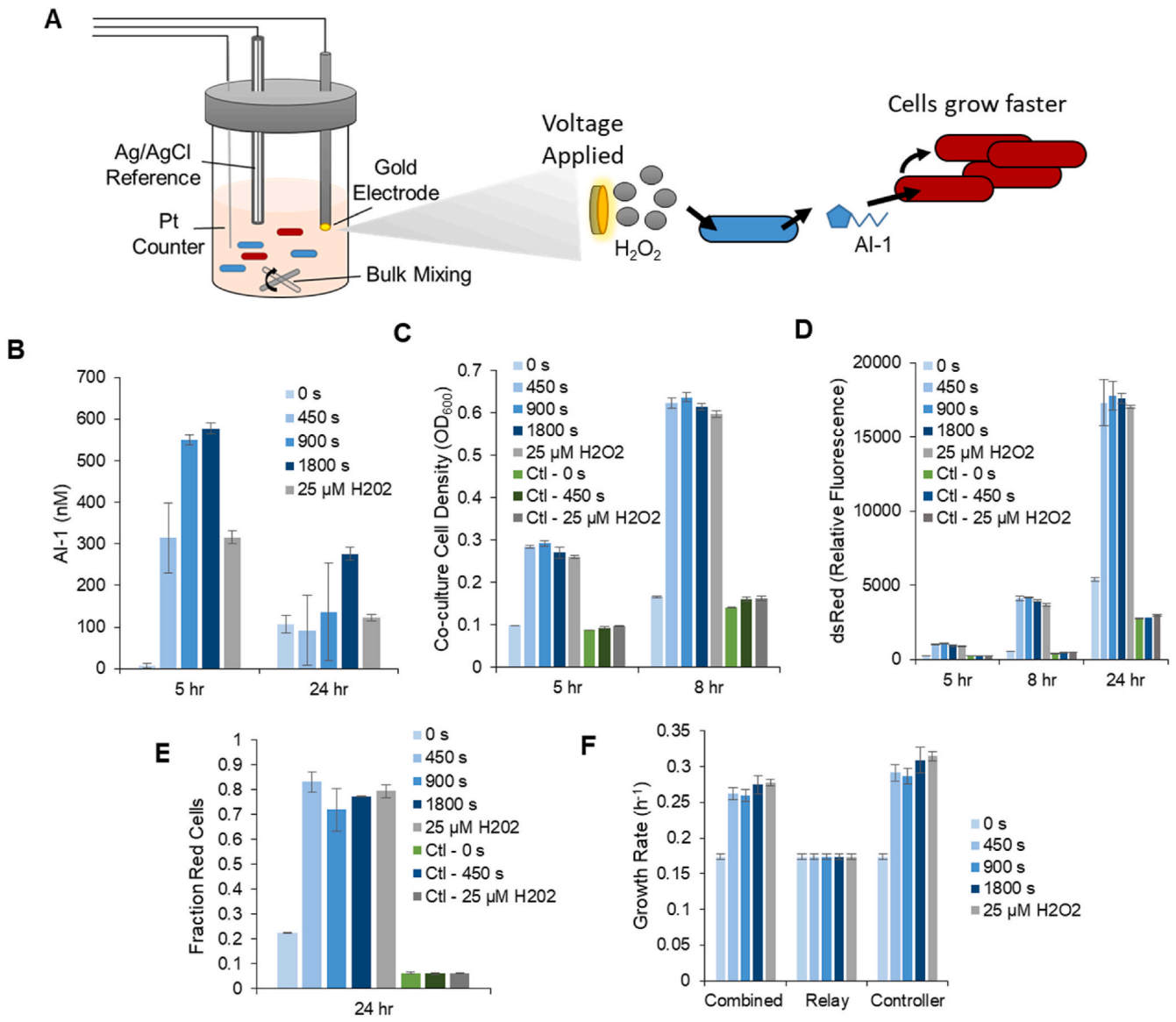

Fig. 4. Electronic control of cell growth rate.
PH04 pOxyRS-LasI (relay cells) and PH04 pAHL-HPr (controller cells) were co-cultured together. The co-cultures were induced at an approximate starting cell density of OD_{600} = 0.05 at a ratio of 4:1 relay to controller cells. A fixed voltage of −0.5 V was applied to the cultures for the amount of time indicated (in seconds). As a positive control, 25 µM hydrogen peroxide was added in place of electric charge. The controls labeled "Ctl" indicate that strain PH04 pCT6 (which does not synthesize AI-1) was used instead of PH04 pOxyRS-LasI to test the effect of charge application or peroxide addition on the co-cultures (independent of AI-1). Time (x-axis) represents the length of time the cultures were incubated after induction. Scheme of experiment (**a**), AI-1 levels (**b**), cell density (**c**), fluorescence measured via a plate reader (**d**), and the fraction of the controller cells measured via microscopy and ImageJ analysis (**e**) are shown. Note that the controller cells constitutively express the fluorescent protein dsRedExpress2. Error bars represent s.d. of biological triplicates.

ptsH gene (encoding HPr) under the AI-1-activated promoter. We previously showed that the growth rate of the controller cells increases with increasing AI-1 (up to about 100 nM AI-1). This strain also constitutively expresses the fluorescent protein dsRedExpress2 so that it can be distinguished from other populations in the culture. HPr is a small, cytoplasmic protein that is involved in uptake of all PTS carbohydrates (as opposed to other PTS enzymes that specifically recognize particular carbohydrates or are associated with the cell membrane) (Deutscher, 2008). PH04 pAHL-HPr and PH04 pOxyRS-LasI were grown initially as monocultures in M9 minimal media to mid-exponential phase. They were then inoculated to a combined starting cell density of approximately OD_{600} 0.05 at a ratio of 4:1 relay to controller cells. The co-cultures were transferred to glass vials for electrical induction (Fig. 4a). A gold electrode (2 mm diameter circle), 4-inch platinum counter wire, and Ag/AgCl reference electrode were inserted into the liquid culture. To electrically induce each culture, a fixed voltage of −0.5 V vs. Ag/AgCl was applied using the gold electrode for a specified amount of time. The applied voltage results in reduction of oxygen at the surface of the electrode and hydrogen peroxide formation (Qiang et al., 2002; Sanchez-Sanchez and Bard, 2009). Increasing the time duration of the applied voltage increases the amount of peroxide generated by the electrode. Electrical induction took place at room temperature, and a stir bar and stir plate were used to continuously mix cultures during induction in order to both maintain the dissolved oxygen availability as well as to distribute the generated peroxide throughout the bulk solution. An experimental condition where 25 µM hydrogen peroxide was added instead of an applied voltage was used as a positive control. After induction, all cultures were transferred to culture tubes and placed in a shaker at 37 °C. We note that this is a modified scheme compared to our previous work. In our previous work (Terrell et al., 2021), the peroxide

detecting cells were adhered to a gold chip. Further, two half-cell reactions were used, where the gold electrode and sample were in one cell and the counter electrode was in a second cell (connected by a salt bridge). Here, the relay cells are in the bulk media with the controller cells and the working and counter electrodes are both in a single cell, negating the requirement for the second cell and salt bridge. We also used a standard gold electrode instead of a larger gold chip. The different schemes may have use for different applications depending on whether the bulk solution can be mixed or whether there is a need to localize different populations in specific spaces.

After electrical induction and incubation of the relay and controller co-cultures, samples were collected for measurement of AI-1, cell density, and culture composition at various time points (Fig. 4b–e). As expected, applying voltage increased AI-1 levels in the culture (measured after 5 h, Fig. 4b). The difference in AI-1 levels between a 900 s and 450 s applied charged was nearly two fold, while increasing the charge length to 1800 s (30 min) did not have a significant additional influence. That said, in all induced cases, sufficient AI-1 was made and secreted to activate a maximal response in the controller cells (>~100 nM).

To confirm increased growth rate in the controller strain, we collected samples of the co-cultures 5 h and 8 h after induction for measurement of cell density (Fig. 4c). We engineered the controller strain to constitutively express a fluorescent marker, dsRed, so that measurement of red fluorescence over time served an indicator of the controller cell fraction within the co-culture (Fig. 4d). At 5 h, induced cultures were observed with increased cell density and, importantly, dsRed expression relative to uninduced cultures. This trend was also observed in samples from 8 h of culture. For the conditions tested, these results appeared to be "on" or "off" rather than a gradient of response; all induced cultures synthesized sufficient AI-1 to fully activate the controller cells. Additional experimental controls were used to test the effect of application of voltage on cell growth and culture composition independent of AI-1 generation (Fig. 4c, **d**, green bars labeled 'Ctl'). In these cultures PH04 pCT6 was used in place of PH04 pOxyRS-LasI as a defective relay population. The plasmid pCT6 was included to maintain ampicillin resistance. In this way, no AI-1 was generated (due to a lack of *lasI*) so that any potential detrimental effects of the applied voltage or hydrogen peroxide generation on cell growth could be assessed. As indicated in Fig. 4c–d, no deleterious effects on either cell growth or culture composition were observed.

After 24 h of culture, we collected final samples and used microscopy and ImageJ to estimate the culture compositions. Electrical activation resulted in a shifted consortia population from less than 25% to over 70% of controller cells (expressing dsRed) compared to cultures where no charge was applied (Fig. 4e). A bulk fluorescence measurement (using a plate reader) was also taken at this point (Fig. 4d) and showed similar trends to the microscopic analyses.

We then calculated the specific growth rate of the cultures using the 5 and 8 h cell density data, and found the cultures with no applied charge had a specific growth rate of 0.17 hr^{-1} compared to a growth rate of 0.27 hr^{-1} for the cultures with an 1800 s applied voltage (Fig. 4f). These are the average specific growth rates for the entire co-culture (accounting for both the relay and controller cells); the differences in growth rate of the controller cells in the induced and un-induced strains accounted for this difference. We estimated the growth rate of the controller cells between the 5 and 8 h marks by assuming that the ratio in the uninduced culture at 5 h was the same as at the start of the experiment (about 20% controller cells) and that the relay population and uninduced controller population grow at the same rate. We found that the controller cells in the population with an 1800 s applied voltage grew about 60% faster than the controller cells in the uninduced population (Fig. 4f). This growth rate increase was similar for the cells induced for shorter times (i.e., 450 & 900 s).

4. Discussion

Electronic modulation of gene expression provides a new avenue for programming and controlling synthetic biology systems. Here, we demonstrate electronic modulation of target gene expression and subsequent biomolecular signal generation to stimulate growth rate of one population in a bacterial co-culture. In this case, we exploit the conversion of an electronically stimulated redox active molecule with limited half-life to a QS autoinducer known to affect cells in mixed cultures and at different length and time scales. That is, the "relay" subpopulation detects the hydrogen peroxide generated by the electrode and produces an AI-1 signal. This signal alters the growth rate of the "controller" strain. We found a significant effect – a 60% increase in the cell growth rate. Electrically induced cultures grew to more than 3 times the cell density after 5 h compared to cultures that were not induced.

We constructed the relay population in a slow-growing host strain (~$\mu = 0.2\ hr^{-1}$ in M9 media), and showed that the relay population was able to produce sufficient AI-1 to activate the controller cells. It is also possible that the relay cells, by producing AI-1 which can diffuse throughout the culture, may allow the controller cells to be activated more uniformly than if HPr was directly modulated by hydrogen peroxide, which is rapidly consumed by the cells nearest the electrode (Virgile et al., 2018). We note that there is likely a steep gradient of hydrogen peroxide within the culture (which is stirred during induction). We expect, however, that the AI-1 signal will persist much longer in the culture, contributing to the sustained and significant changes observed in cell growth rate.

Interestingly, the data shown here suggest a robust "on/off" switch, more so than finely tuned control that might generate an intermediate growth rate at intermediate levels of signal generation. This "on/off" attribute can be a strength in that one could employ a separate control variable to depress growth rate, rather than focus on developing a more sophisticated genetic circuit within the engineered cell that would "hit" the intended growth rate based on the prevailing signal molecule concentration. The latter is particularly challenging in that the initial signal molecule concentration perceived by the cell determines the future genetically-encoded trajectory of that cell (Servinsky et al., 2016; Ueda et al., 2019). Further, this process is often characterized by long time constants, longer than those that could change the extracellular signal molecule concentration. Indeed, other control variables could be employed in parallel with a modified genetic circuit, to enable more rapid response, such as dilution. We suggest that by incorporating electronics, one can more easily control a complex biological system, wherein one accommodates the overall process time constants rather than the dynamics of a specific genetic circuit. The utility of an electrogenetic "on/off" switch can be envisioned by the analogous "on/off" thermostat that controls the temperature in a house (that may take a long (or short) time to heat or cool based on the prevailing conditions).

In sum, we believe there is great utility for electronically modulating cell growth rate, an additional feature to our earlier work showing electronic actuation of gene expression (Tschirhart et al., 2017). We anticipate wide ranging applicability for this concept. Consider application in microfluidic systems, such as animal-on-a-chip devices, where controlled cell growth rate would be advantageous but has yet to be reported. To alter growth rate, one would typically alter nutrient levels and because fluids are spatially segregated, additional serpentine mixing modules, pumps, valves, etc, would be needed. Instead, the placement of an electrode that spans the width of a microfluidic channel could, at one time, stimulate all cells in that channel and in a specific region of that channel. By extension and by incorporating the results here, one could potentially modulate the growth rate of a *specific* strain within a microbial community and at a specific site, thereby guiding a population of cells to perform complex functions. In turn, complex microbiomes, where consortia provide for homeostasis might be a target. For example, ingested miniaturized devices, such as "smart" pills, are now integrating constructs of synthetic biology (Mimee et al., 2018). Mimee et al.

demonstrated *in vivo* application of an ingestible pill containing heme-detecting bacteria (Mimee et al., 2018). A next step might be signal or therapeutic delivery from other resident electronically-cued bacteria, or alteration of nearby strains within the microbiome that are engineered to receive signals from the pill. We anticipate both increased application of electrogenetic control and increased complexity of synthetic biology constructs in similar devices for diagnosis and treatment of disease, particularly in complex environments like the GI tract where modulation of chemical signaling is extremely difficult. Technologies for electronic actuation of gene expression, or control of cell growth rate, as demonstrated here, would complement methodologies designed for electronic reporting of gene expression (Tschirhart et al., 2016), or population size (Din et al., 2020). Additional applications might be in wound healing, regenerative medicine, and immunotherapy, as well as in areas beyond human health including environmental security and food production.

5. Materials and methods

5.1. Strains and plasmids

Strains, plasmids, and primers used in this study are listed in Supplementary Tables 1 and 2 Plasmid pOxyRS-LasI (Terrell et al., 2021) is derived from pOxyRS-LacZ-ssRA. Gibson Assembly (New England Biolabs) was used to insert LasI-ssRA in place of LacZ-ssRA. Primers OxySv2Assem-R, ssRA-F, OxySv2-LasI-F, and LasI-ssRA-R were used to amplify the vector and insert for pOxyRS-LasI.

5.2. Cell culture conditions

Cultures were incubated at 37 °C with 250 rpm shaking. Prior to each experiment, strains were inoculated into LB media from glycerol stocks. After overnight growth, cultures were then re-inoculated into in M9 minimal media (1x M9 salts, 2 mM $MgSO_4$, 0.1 mM $CaCl_2$, 0.2%, 0.4% glucose) and grown for at least 1 h. Then, cultures or co-cultures were re-inoculated into M9 minimal media at the desired starting cell densities for the experiments. During electronic induction, all cultures remained at room temperature. After induction, cultures were moved to the incubator. Media contained 50 μg/mL ampicillin to maintain plasmids.

5.3. Electrochemical setup for hydrogen peroxide generation

For electrochemical induction of cultures, 1 mL cultures were placed in a closed glass vial (17 × 60 mm, Fisher Scientific). The gold standard electrode (2 mm diameter, CH Instruments), a 4-inch counter platinum wire (Alfa Aesar), and Ag/AgCl reference electrode (BASi) were secured by punctured holes in the vial cap. To begin the reaction, the electrodes were positioned near the surface of the liquid culture and biased to −0.5 V vs. Ag/AgCl for variable times. The oxygen reduction current was measured over time to monitor the reaction (generation of hydrogen peroxide). Each sample was continuously stirred using a stir bar. After completion of induction, the culture was transferred to a culture tube before being moved to a 37 °C shaker.

5.4. Measurement of AI-1

Cell-free experimental conditioned media samples were collected by filtering samples through a 0.2 μM filter. Samples were stored at −20 °C until ready for AI-1 analysis. AI-1 was measured using a luminescent reporter assay, as performed previously (Stephens et al., 2019). *E. coli* reporter cells containing plasmid pAL 105 (Lindsay and Ahmer, 2005) were grown overnight in LB media. Overnight reporter cells were diluted 2500x in LB media. The experimental samples were thawed and diluted 5x in LB media. Standard curve samples consisting of 0, 12, 24, 36, 48, and 60 nM AI-1 in LB media were generated. 10 μL of experimental or standard curve sample were added to 90 μL of reporter cells in flow cytometry culture tubes. After 3 h of growth at 30 °C, 250 rpm shaking, luminescence values were recorded (Promega GloMAX luminometer). The standard curve was used to calculate the AI-1 level in the assay, and then this number was multiplied by the dilution factor to estimate the AI-1 concentration in the original experimental sample.

The experiment shown in Fig. 3 used a slightly modified reporter assay where luminescence was measured using a plate reader (Tecan Spark multimode microplate reader, with a 500 ms integration time). The overnight reporter cells were diluted 100x in LB media. 20 μL of experimental sample (diluted 5x) or standard curve sample were added to 180 μL of reporter cells in a white wall/white bottom 96-well plate. Calculation of AI-1 was again based on the standard curve, which was run in parallel with the experimental samples, so results are comparable between the original and modified assay.

5.5. Measurement of dsRed fluorescence

A SpectraMax M2e plate reader was used to measure bulk dsRed fluorescence in the experimental samples. 200 μL samples were collected from experimental cultures and added to a black wall, clear bottom, 96-well plate. 550 nm and 579 nm were used for the excitation and emission wave lengths, respectively, with a cutoff of 570 nm.

Microscopy and ImageJ were used to estimate the fraction of dsRed-expressing cells in the cultures, using a previously developed method (Stephens et al., 2019). Briefly, for each sample, bright field images and fluorescent images were taken at four different locations. ImageJ was used to count the cells in the bright field images and the cells in the fluorescent images. The reported fraction is the fluorescent image cell count divided by the bright field image cell count, multiplied by a factor of 1.18. This factor accounts for an undercount of red cells using this method and is based on previous work developing the method.

CRediT authorship contribution statement

Kristina Stephens: Conceptualization, Data curation, Formal analysis, Investigation, Methodology, Project administration, Software, Validation, Visualization, Roles/Writing. **Fauziah Rahma Zakaria:** Conceptualization, Data curation. **Eric VanArsdale:** Conceptualization. **Gregory F. Payne:** Conceptualization, Data curation, Formal analysis, Funding acquisition, Methodology, Project administration, Resources, Supervision, Validation, Visualization, Roles/Writing. **William E. Bentley:** Conceptualization, Data curation, Formal analysis, Funding acquisition, Methodology, Project administration, Resources, Software, Supervision, Validation, Visualization, Roles/Writing.

Declaration of interests

The authors declare that they have no known competing financial interests or personal relationships that could have appeared to influence the work reported in this paper.

Acknowledgements

The authors would like to acknowledge the following sponsors for support of this work: The National Science Foundation (#CBET1805274, #ECCS1807604, #CBET1932963), The Defense Threat Reduction Agency (HDTRA1-19-1-0021), Department of Energy (BER#SCW1710).

Appendix A. Supplementary data

Supplementary data to this article can be found online at https://doi.org/10.1016/j.mec.2021.e00176

References

Andersen, J.B., et al., 1998. New unstable variants of green fluorescent protein for studies of transient gene expression in bacteria. Appl. Environ. Microbiol. 64, 2240–2246.

Bhokisham, N., et al., 2020. A redox-based electrogenetic CRISPR system to connect with and control biological information networks. Nat. Commun. 11, 2427.

Cai, S., et al., 2018. Engineering highly sensitive whole-cell mercury biosensors based on positive feedback loops from quorum-sensing systems. Analyst 143, 630–634.

Cameron, D.E., Bashor, C.J., Collins, J.J., 2014. A brief history of synthetic biology. Nat. Rev. Microbiol. 12, 381–390.

Deutscher, J., 2008. The mechanisms of carbon catabolite repression in bacteria. Curr. Opin. Microbiol. 11, 87–93.

Dietrich, L.E., Teal, T.K., Price-Whelan, A., Newman, D.K., 2008. Redox-active antibiotics control gene expression and community behavior in divergent bacteria. Science 321, 1203–1206.

Din, M.O., Martin, A., Razinkov, I., Csicsery, N., Hasty, J., 2020. Interfacing gene circuits with microelectronics through engineered population dynamics. Sci. Adv. 6, eaaz8344.

Ha, J.H., et al., 2018. Evidence of link between quorum sensing and sugar metabolism in Escherichia coli revealed via cocrystal structures of LsrK and HPr. Sci. Adv. 4, eaar7063.

Hwang, I.Y., et al., 2017. Engineered probiotic Escherichia coli can eliminate and prevent Pseudomonas aeruginosa gut infection in animal models. Nat. Commun. 8, 15028.

Jawed, K., Yazdani, S.S., Koffas, M.A., 2019. Advances in the development and application of microbial consortia for metabolic engineering. Metab. Eng. Comm. 9, e00095.

Kang, Y., et al., 2018. Enhancing the copper-sensing capability of Escherichia coli-based whole-cell bioreporters by genetic engineering. Appl. Microbiol. Biotechnol. 102, 1513–1521.

Krawczyk, K., et al., 2020. Electrogenetic cellular insulin release for real-time glycemic control in type 1 diabetic mice. Science 368, 993–1001.

Lindsay, A., Ahmer, B.M., 2005. Effect of sdiA on biosensors of N-acylhomoserine lactones. J. Bacteriol. 187, 5054–5058.

McKay, R., et al., 2017. Controlling localization of Escherichia coli populations using a two-part synthetic motility circuit: an accelerator and brake. Biotechnol. Bioeng. 114, 2883–2895.

McKay, R., et al., 2018. A platform of genetically engineered bacteria as vehicles for localized delivery of therapeutics: toward applications for Crohn's disease. Bioengineering & translational medicine 3, 209–221.

Miller, M.B., Bassler, B.L., 2001. Quorum sensing in bacteria. Annu. Rev. Microbiol. 55, 165–199.

Mimee, M., et al., 2018. An ingestible bacterial-electronic system to monitor gastrointestinal health. Science 360, 915–918.

Olson, E.J., Hartsough, L.A., Landry, B.P., Shroff, R., Tabor, J.J., 2014. Characterizing bacterial gene circuit dynamics with optically programmed gene expression signals. Nat. Methods 11, 449–455.

Qiang, Z., Chang, J.H., Huang, C.P., 2002. Electrochemical generation of hydrogen peroxide from dissolved oxygen in acidic solutions. Water Res. 36, 85–94.

Roggo, C., van der Meer, J.R., 2017. Miniaturized and integrated whole cell living bacterial sensors in field applicable autonomous devices. Curr. Opin. Biotechnol. 45, 24–33.

Rubens, J.R., Selvaggio, G., Lu, T.K., 2016. Synthetic mixed-signal computation in living cells. Nat. Commun. 7, 11658.

Sanchez-Sanchez, C.M., Bard, A.J., 2009. Hydrogen peroxide production in the oxygen reduction reaction at different electrocatalysts as quantified by scanning electrochemical microscopy. Anal. Chem. 81, 8094–8100.

Servinsky, M.D., et al., 2016. Directed assembly of a bacterial quorum. ISME J. 10, 158–169.

Stanley, S.A., Sauer, J., Kane, R.S., Dordick, J.S., Friedman, J.M., 2015. Remote regulation of glucose homeostasis in mice using genetically encoded nanoparticles. Nat. Med. 21, 92–98.

Stephens, K., Pozo, M., Tsao, C.Y., Hauk, P., Bentley, W.E., 2019. Bacterial co-culture with cell signaling translator and growth controller modules for autonomously regulated culture composition. Nat. Commun. 10, 4129.

Terrell, J.L., et al., 2021. Bioelectronic control of a microbial community using surface-assembled electrogenetic cells to route signals. Nat. Nanotechnol. 16 (6), 688–697.

Tsaneva, I.R., Weiss, B. soxR., 1990. A locus governing a superoxide response regulon in Escherichia coli K-12. J. Bacteriol. 172, 4197–4205.

Tschirhart, T., et al., 2016. Electrochemical measurement of the beta-galactosidase reporter from live cells: a comparison to the miller assay. ACS Synth. Biol. 5, 28–35.

Tschirhart, T., et al., 2017. Electronic control of gene expression and cell behaviour in Escherichia coli through redox signalling. Nat. Commun. 8, 14030.

Ueda, H., Stephens, K., Trivisa, K., Bentley, W.E., 2019. Bacteria floc, but do they flock? Insights from population interaction models of quorum sensing. mBio 10.

Virgile, C., et al., 2018. Engineering bacterial motility towards hydrogen-peroxide. PloS One 13, e0196999.

Weber, W., et al., 2009. A synthetic mammalian electro-genetic transcription circuit. Nucleic Acids Res. 37, e33.